Available online at www.sciencedirect.com

SciVerse ScienceDirect

Ceramics International 39 (2013) 289–297

CERAMICS INTERNATIONAL

www.elsevier.com/locate/ceramint

Biological response of a recently developed nanocomposite based on calcium phosphate cement and sol–gel derived bioactive glass fibers as substitution of bone tissues

Nader Nezafati[a], Fathollah Moztarzadeh[a], Saeed Hesaraki[b], Zoha Moztarzadeh[c], Masoud Mozafari[a,d,*]

[a]*Biomaterials Group, Faculty of Biomedical Engineering (Center of Excellence), Amirkabir University of Technology, PO Box 15875-4413, Tehran, Iran*
[b]*Nanotechnology and Advanced Materials Department, Materials and Energy Research Center, PO Box 31787-316, Karaj, Iran*
[c]*Institute of Bioinformatic, Münster University, Münster, Germany*
[d]*Helmerich Advanced Technology Research Center, School of Material Science and Engineering, Oklahoma State University, OK 74106, USA*

Received 17 April 2012; received in revised form 1 June 2012; accepted 6 June 2012
Available online 20 June 2012

Abstract

Calcium phosphate cements (CPCs) have been used in a number of medical and dental procedures due to their excellent osteoconductivity and bone replacement capability. However, the low mechanical properties of CPCs prohibit their usage in many unsupported defects and stress bearing locations. Bioactive glass fiber (BGF) reinforced-CPC with enhanced mechanical property has been recently developed [Nezafati et al. 2011, Ceramics International]. In the present study, the in vitro bioactivity and cellular properties of the CPC optimally reinforced with 15 vol% BGFs were evaluated and compared with a control group, i.e. unreinforced CPC. The samples were soaked in simulated body fluid (SBF) for different time intervals and were then characterized by various techniques. Carbonate substituted apatite crystals with oriented plate-like morphology were also found on the surface of the samples. Furthermore, rat-derived osteoblastic cells were seeded on the samples for different times and evaluated in terms of proliferation, morphology and alkaline phosphatase (ALP) activity. In addition, the proliferation of osteoblastic cells on samples and increasing in level of alkaline phosphatase enzyme were observed as a function of time. The obtained results indicated that the reinforced composite made of CPC and BGFs could be considered as a highly bioactive material for bone tissue defect treatment after successful passage of *in vivo* experiments.

Keywords: Calcium phosphate cement; Bioactive glass fiber; *In vitro* bioactivity; Bone-like apatite

1. Introduction

In recent years, many inorganic bioactive materials have been studied for the repair and filling of bone defects and as scaffolds for tissue engineering. They include calcium phosphate ceramics, hydroxyapatite (HAp) ceramic, bioactive glass (BG) and calcium phosphate cements (CPC). HA, CPC and BG are usually considered bone bioactive ceramics, implying that they bond to surrounding osseous tissue and enhance bone tissue formation [1].

CPCs are highly promising for use in a wide range of biomedical applications, due to their osteoconductivity and bone replacement capability [2]. This type of material has a higher resorption rate than HA and it is normally considered as a biodegradable material that allows bone growth and replacement. Like to HA, CPC is also weak in mechanical strength and should be reinforced before implantation. In addition, CPC has a nearly poor ability for inducing calcium phosphate precipitation both *in vitro* and *in vivo*, so it cannot be perfectly bonded to living

*Corresponding author at: Helmerich Advanced Technology Research Center, School of Material Science and Engineering, Oklahoma State University, OK 74106, USA. Tel.: +1 918 594 8634; fax: +1 270 897 1179.
E-mail address: masoud.mozafari@okstate.edu (M. Mozafari).

0272-8842/$36.00
http://dx.doi.org/10.1016/j.ceramint.2012.06.024

tissues. Sol–gel derived bioactive glasses are also appropriate candidate to be incorporated with CPC, because of their high surface area and their unique bioactivity [3]. In this context, numerous studies of in vitro bioactivity have been carried out for BGs obtained by the sol–gel method, belonging to different systems such as $CaO–P_2O_5–SiO_2$ [4], $CaO–MgO–P_2O_5–SiO_2$ [5,6] and $CaO–SiO_2$ [7]. These assays revealed that the immersion of glasses in SBF led to increasing Ca^{2+} concentration and pH due to a partial solution of glass network. Obviously, these changes affected the layer formation rate and solid–liquid interaction. In addition, BG could elicit a specific biological *in vivo* response at the interface and attach to the tissues, such as soft tissue and bone with a strong chemical bond. So they have been widely used for a number of different biomedical applications. Certain compositions of BGs containing $SiO_2–CaO–P_2O_5$ bonded to both soft and hard tissue without an intervening fibrous layer. Results of *in vivo* implantation showed that these compositions produced no local or systemic toxicity, no inflammation, and no foreign-body response [8,9].

To solve the weakness of CPC, different kinds of fibers have been widely used to improve the strength and fracture resistance of them [10–14]. Ideal tissue engineering materials should be biocompatible and highly bioactive with adequate mechanical properties. For this purpose, in our previous work [15] CPC/BGFs composites were mechanically optimized, and herein, the samples were evaluated *in vitro*.

Briefly, the prepared composites were tested to determine the effects of using the BGFs on the mechanical properties of the samples. The compressive strength, elastic constant and work-of-fracture values of the composites containing 5 and 15% BGFs were considerably higher than the un-reinforced cement while the values of the composite containing 25% BGFs were significantly lower than the sample containing 5% BGFs. It could be also observed that applying the larger amounts of admixture not only increased the mechanical properties of CPC but also acted as defect sites in the cement's microstructure and decreased the mechanical properties of the prepared samples. It is important to point out that the mechanical properties of the composite samples were generally higher than the un-reinforced cement (control sample). Basically, as a fundamental rule, unlike unidirectional fiber-reinforced composites whose mechanical properties show a continuous increase with an increase in fiber volume fraction, the modulus and strength of the random fiber composites increase with fiber volume fraction up to a certain maximum value and then start to decrease. Herein, the optimum mechanical properties obtained for the sample containing 15% BGF.

Hence, in the present research, the *in vitro* bioactivities of the mechanically optimized composite sample in SBF were investigated in detail. In addition, osteoblastic cells were seeded on the samples for different times and evaluated in terms of proliferation, morphology and alkaline phosphatase activity. The proliferation of osteoblastic cells on cements and increasing in level of alkaline phosphatase enzyme were also observed as a function of time. We hypothesized that such CPC/BGFs composite would provide excellent biocompatibility as well as enhanced mechanical properties.

2. Materials and methods

2.1. Preparation of the BGFs

The sol–gel derived BGFs were prepared according to the following procedure. In short, TEOS was added to a water–ethanol solution (pH = 1.5, adjusted with HCl) at a molar ratio of 2:1 for water/TEOS and 4:1 for ethanol/TEOS. The mixture was stirred for 1 h at room temperature. The TEP was added to the silica sol, which was stirred for another 1 h. Calcium nitrate was then introduced to the sol and the mixture was stirred for an additional hour. The resultant sol was stirred at 50 rpm by concentrating the sol through solvent removal at 293 K. The condensation process was terminated when the viscosity of the solution was sufficient for fiber pulling (until viscosities near 4–5 Pa-s were achieved). The fiber-shaped gel was produced by extruding the viscous gel through a thin syringe with needle's inside diameter of 0.01 mm. The fibers were cut with sharp surgical blades into filaments of length 2–3 mm. However, due to the brittle nature of BGFs the actual length would be random after mixing with CPC. Fibers were then dried for 24 h at 343 K. Finally, they were then heated to 973 K at an approximate rate of 3 K min^{-1} and then sintered and stabilized at 973 K for 24 h.

2.2. Preparation of the CPC

First, TTCP powder was synthesized by a combination of 1 mol of DCPD and 1 mol of $CaCO_3$ after milling for 2 h. Then, it was heated to 1773 K (in an alumina crucible) at an approximate rate of 7 K min^{-1} and maintained for 5 h at the same temperature. After that, it was extracted immediately, cooled at room temperature and ground in a planetary mill to an average particle size of 12 μm (Fritsch particle sizer analysette 22). A mixture of DCPD (average particle size of 6 μm) and TTCP, in a molar ratio of 1:1, was used as the solid phase of the cement. The liquid phase was a solution of 6 wt% Na_2HPO_4. The cement paste was made by mixing the powder to the liquid phase at powder to liquid ratio of 3 g/ml.

2.3. Preparation of the CPC/BGF composite

The preparation method of composite samples was previously described by Nezafati et al. [29]. Briefly, to prepare CPC/BGF composites, the obtained BGFs were mixed with the cement powder at various weight ratios of 5, 15 and 25% (based on the whole weight of the powder and liquid) and then the liquid phase was added to the

mixture to obtain a paste. Note that the weight of the glassy fibers was not considered in the Powder-to-Liquid (P/L) calculations.

2.4. Preparation of SBF solution

In this study, conventional SBF (c-SBF) prepared according to the Kokubo's specification was used [16]. The SBF solution was prepared by dissolving reagent-grade NaCl, KCl, $NaHCO_3$, $MgCl_2$ $6H_2O$, $CaCl_2$ and KH_2PO_4 into distilled water and buffered at pH = 7.25 with TRIS (trishydroxymethyl aminomethane) and 1 N HCl solution at 310 K. The SBF was refreshed every 24 h in order to mimic the fluid circulation in human body. According to Oyane and Takadama, the SBF solution is so far the best solution for *in vitro* measurement of apatite-forming ability in implant materials. The SBF solution was chosen because of its highly supersaturated characteristic with respect to apatite [17,18].

2.5. Sample characterization

2.5.1. SEM analysis

The morphology and microstructure of the prepared composite samples were evaluated using SEM. The composite samples were coated with a thin layer of Gold (Au) by sputtering (EMITECH K450X, England) and then the morphology of them were observed on a SEM-Philips XL30 that operated at the acceleration voltage of 15 kV.

2.5.2. XRD analysis

The samples surfaces were analyzed by XRD with Siemens-Brucker D5000 diffractometer. This instrument works with voltage and current settings of 40 kV and 40 mA respectively and uses Cu-Kα radiation (1.540600 Å). For qualitative analysis, XRD diagrams were recorded in the interval $10^\circ \leq 2\theta \leq 50^\circ$at scan speed of 2°/min.

2.5.3. FTIR analysis

The samples were examined by FTIR with Bomem MB 100 spectrometer. For IR analysis, at first 1 mg of the scraped samples were carefully mixed with 300 mg of KBr (infrared grade) and palletized under vacuum. Then the pellets were analyzed in the range of total number of scans at the scan speed of 23 scan/min with 4 cm^{-1} resolution.

2.5.4. EDX analysis

Energy dispersive X-ray analyzer (EDX, Rontec, Germany) connected to SEM was used to investigate semi-quantitatively chemical compositions.

2.6. In vitro biomineralization study in SBF solution

We carried out *in vitro* studies by soaking the samples in SBF solution at 37 °C for 14 day. At regular intervals (1, 3 and 7 days) samples were taken out and before the analysis of the soaked specimens, they were washed carefully with distilled water, dried at room temperature, crushed in an agate mortar and tested by FTIR, SEM, EDX and XRD.

2.7. Cellular responses to the composite samples

To evaluate the biological properties of samples, osteoblastic cells were derived from newborn rat calvaria and isolated by sequential collagenase digestion from calvaria of newborn (2–5 day) Wistar and cultured in Dulbecco modified Eagle medium (DMEM; Gibco-BRL, Life Technologies, Grand Island, NY) supplemented with 15% fetal bovine serum (FBS; Dainippon Pharmaceutical, Osaka, Japan) and 100 g/mL penicillin–streptomycin (Gibco-BRL, Life Technologies) in a 5% CO_2/95% air atmosphere at 37 °C for 1 week. The medium was changed every 2 day. The confluent cells were dissociated with trypsin and subcultured to 3 passages which were used for tests.

Then, the disk-shaped cement specimens (6 mm in diameter and 3 mm in height) were sterilized using 70% ethanol and the rat calvaria-derived osteoblastic cells extracted and passaged according to previously described method [19] were seeded on tops of the glass disks at 1×10^4 cells/disk. The specimen/cell samples were placed into 24-wells culture plates and left undisturbed in an incubator for 3 h to allow the cells to attach to them and then an additional 3 ml of culture medium was added into each well. The cell/specimen constructs were cultured in a humidified incubator at 37 °C with 95% air and 5% CO_2 for 1,7, and 14 day. Note that, every 3 day, the medium was exchanged.

The proliferation of the osteoblastic cells on bioactive glass specimens was determined using the MTT (3-{4,5-dimethylthiazol-2yl}-2,5-diphenyl-2H-tetrazolium bromide) assay. For this purpose, at the end of each evaluating period, the medium was removed and 2 ml of MTT solution was added to each well. Following incubation at 37 °C for 4 h in a fully humidified atmosphere at 5% CO_2 in air, MTT was taken up by active cells and reduced in the mitochondria to insoluble purple formazan granules. Subsequently, the medium was discarded and the precipitated formazan was dissolved in dimethylsulfoxide, DMSO, (150 ml/well), and optical density of the solution was read using a microplate spectrophotometer (BIO-TEK Elx 800, Highland park, USA) at a wavelength of 570 nm.

To observe the morphologies of the cells attached onto the surfaces of the glass specimens, the cells were cultured onto the glass disks as described above. After 14 day, the culture medium was removed, the cell-cultured specimens were rinsed with phosphate buffered saline (PBS) twice and then the cells were fixed with 500 mL/well of 3% glutaraldehyde solution (diluted from 50% glutaraldehyde solution (Electron Microscopy Science, USA) with PBS). After 30 min, they were rinsed again and kept in PBS at 4 °C. Specimens were then fixed with 1% Osmium tetroxide (Polyscience, Warmington, PA, USA). After cell fixation, the specimens were dehydrated in ethanol solutions of

varying concentration (30, 50, 70, 90, and 100%) for about 20 min at each concentration. The specimens were then dried in the air, coated with gold and analyzed by SEM. Cellular responses were scored as 0, 1, 2 and 3 according to non-cytotoxic, mildly cytotoxic and severely cytotoxic as per ISO 10993–5.

2.8. ALP activity

The osteoblast activity was determined by measuring the level of alkaline phosphatase enzyme. The cells were seeded on the samples under the same culturing condition described elsewhere and the level of ALP was determined on days 1, 7 and 14. The osteoblasts lysates were frozen and thawed three times to disrupt the cell membranes. ALP activity was determined at 405 nm using p-nitrophenyl phosphate in diethanolamide buffer as chromogenic substrate.

2.9. Statistical analysis

All experiments were performed in fifth replicate. The results were given as means ± standard error (SE). Statistical analysis was performed by using One-way ANOVA and Tukey test with significance reported when $P < 0.05$. Also for investigation of group normalizing, Kolmogorov–Smirnov test was used.

3. Results and discussion

3.1. SEM observations of the prepared composites

Fig. 1(a) and (b) show a typical optical photo of the lateral view of the prepared composite containing 15% BGFs, and the SEM micrograph captured from the top view of samples showing the BGFs that were randomly mixed with the CPC paste, respectively. Fig. 1 revealed that the adhering of cement particles to the surfaces of fibers and also possibly adhering of these components. As it can be seen in this figure, the presence of some pellicles may cause coupling of the fibers to the CPC matrix. According to the observations, no micrographs of surface fractures even with the unaided eyes could be seen indicating that the BGFs became anchored and coupled to the CPC matrix and thus preventing the cement from disintegrating. It is important to point out with respect to Dos Santos et al. [20], in clinical applications, keeping fragmented parts of cement together is useful in order to prevent them from migrating to soft tissues and causing undesirable reactions. Moreover, bone tissue may migrate into fractures in the material, resulting in greater osteointegration of the implanted material.

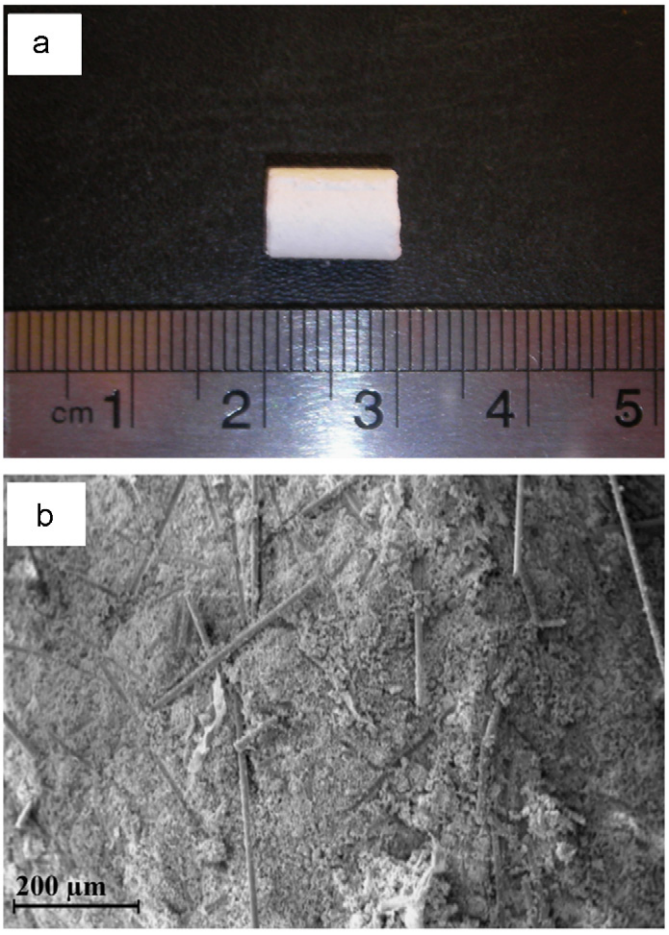

Fig. 1. (a) Optical photo and (b) SEM micrograph of the prepared composite containing 15% BGFs that were randomly mixed with the CPC paste.

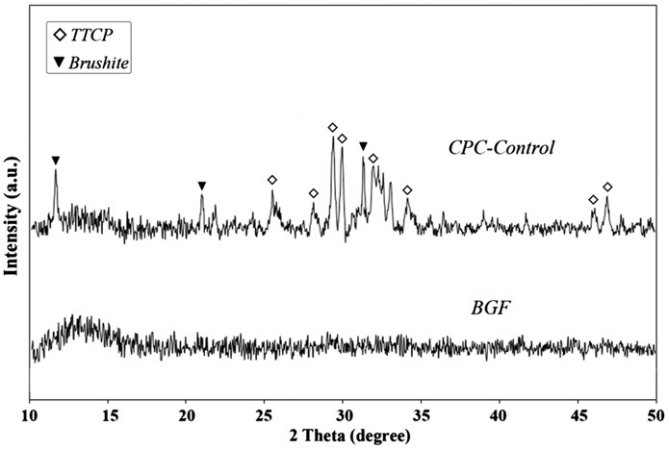

Fig. 2. The XRD patterns of (a) the prepared BGFs, (b) the CPC (unreinforced cement).

3.2. XRD analysis

The phase purity and phase structure of the synthesized BGF and the CPC (unreinforced cement) were characterized by XRD which are shown in Fig. 2. In the BGF pattern, the sample almost took amorphous state which indicated the internal disorder and glassy nature of these materials. It is worth mentioning that the BGF did not show any crystalline states after heat-treatment at 973 K [21,22].

For the CPC sample, a considerable amount of the reactant phase in the cement composition was observed. The apatite phase was also observed in the composition (apatite is the product of the setting reaction). The setting mechanisms of CPCs are so complicated that have not been identified completely but there are some hypotheses about setting phenomena of them. The main reason for the setting process of CPCs is the precipitation of different phases such as brushite, apatite or octacalcium phosphate in the cement paste [23]. Herein, brushite and TTCP could also be seen in the XRD patterns.

In apatitic calcium phosphate cements, the presence of the initial crystals of apatite is due to the dissolution of tetra-calcium phosphate particles and their hydrolysis to stoichiometric hydroxyl apatite as follows (4):

$$Ca_4(PO_4)_2 + H_2O \rightarrow Ca_{10}(PO_4)_6(OH)_2 + Ca(OH)_2 \quad (4)$$

In addition, the growth of apatite crystals is because of the acidic-basic reaction as follows (5) [23]:

$$3Ca_4(PO_4)_2O + 6CaHPO_4 \rightarrow 2Ca_2(HPO_4)(PO_4)_5OH + H_20 \quad (5)$$

The setting process was being gradually continued and completed after a period of time and the cross-linking process of ions, so as to cause cement strength. There are different parameters which affect the setting time of CPCs and consequently increase their strength, including the composition of material used in the liquid/solid phase, the powder-to-liquid ratio and particle size of the reactants [24].

3.3. In vitro assays in SBF environment

Generally, HAp is a naturally occurring mineral and the predominant mineral component of vertebrate bone and tooth enamel. Naturally-occurring bone mineral is made of nanometer sized, poorly-crystalline calcium phosphate with HAp structure. However, speaking of the ideal stoichiometric crystalline HAp $Ca_{10}(PO_4)_6(OH)_2$ with atomic Ca/P ratio 1.67 [25,26], and the composition of bone mineral are significantly different and may be represented by the following formula (6):

$$Ca8.3(PO_4)4.3(HPO4,\ CO3)_{1.7}(OH,\ CO_3)_{0.3} \quad (6)$$

Bone mineral non-stoichiometry is primarily due to the presence of divalent ions, such as CO_3^{2-} and HPO_4^{2-} which are substituted for the trivalent PO_4^{3-} ions. Substitution by CO_3^{2-} and HPO_4^{2-} ions produce a change of Ca/P ratio, resulting in the Ca/P ratio which may vary between 1.50 and 1.70 depending on the age and bone site [26].

It is also important to point out that, one of the essential conditions for biomaterials to bond with living bone is the formation of a surface apatite layer in the body environment. To determine the bioactivity of the materials, the composites were subjected to in vitro solution testing using SBF solution. The samples were immersed in SBF at 310 K for 1, 3, and 7 day. Fig. 3 shows the FTIR spectra of the composite sample containing 15% BGF before and after immersion in SBF for different periods of time. After immersion at various times in SBF solution, additional peaks appeared in the FTIR spectra, for example the bands at 1000 and 600 cm^{-1} arise from υ_3 PO_4 and υ_4 PO_4, respectively [27], indicated apatite formation on the surface of immersed samples in the SBF solution.

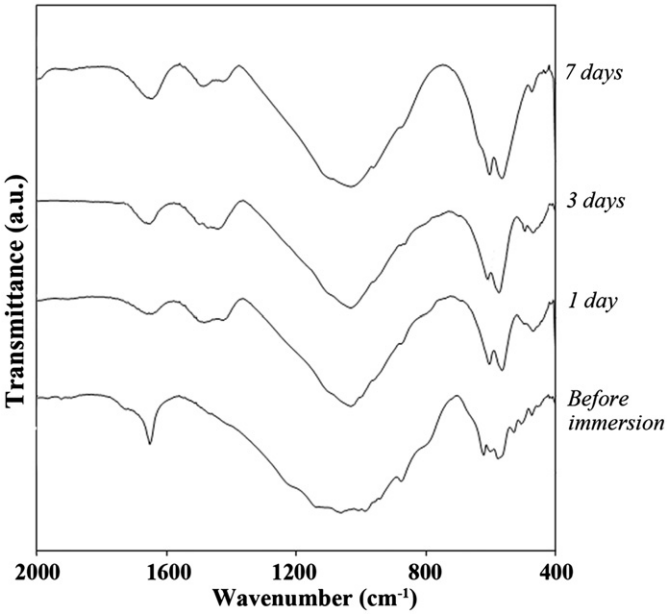

Fig. 3. The FTIR spectra of the grinded composite sample containing 15% BGFs before and after immersion in SBF for different periods of time.

In addition, the FTIR analyses revealed that the spectra of the sample after immersion in SBF for 7 day showed changes in its appearance in comparison to the spectra of samples before immersion. Absorption bands located at 870 cm^{-1} (C–O bond) and 960 cm^{-1} (P–O symmetric stretch, characteristic of HCAp), indicated that this phase was typically related to poorly crystallized carbonate apatite. Moreover, bands located at 1470 and 1533 cm^{-1} also appeared which could be assigned to $\nu_3 CO_3^{2-}$. According to the explanations, the appearance of these new carbonate bands confirmed the formation of bone-like apatite onto the surface of composite samples.

In order to further improve the mechanical strength of the composites and enhance osteoblasts differentiation, bone-like apatite was incorporated onto the surface of bioactive materials in body environment. According to Mozafari et al. [28] formation of bone-like apatite on the surface of these kinds of bioactive composites may improve the mechanical strength and enhance osteoblast differentiation. Herein, apatite was incorporated onto the surface of the composites in situ via using the SBF technique. Fig. 4 shows SEM micrographs of the composite sample containing 15% BGFs before and after immersion for 1, 3 and 7 day in SBF solution. According to the observations, scattered and small particles were covered on the surface of the composite surfaces after

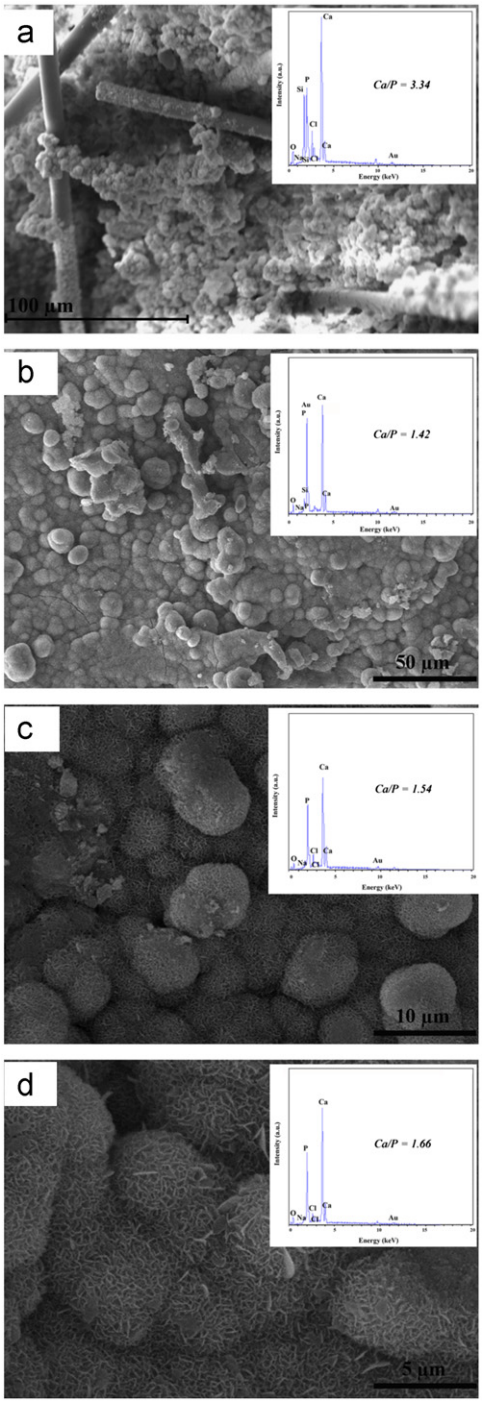

Fig. 4. The SEM micrographs and EDX patterns of the composites before (a), and after immersion in SBF for 1 day (b), 3 day (c) and 7 day (d).

1 day of immersion which is shown in Fig. 4(b). After 3 day, substantial amount of apatite microparticles formed on the surfaces of the samples as shown in Fig. 4(c). Subsequently, after 7 day of immersion, the whole surfaces of the samples were covered by a layer of apatite, and the underlying surfaces were not clearly observable. According to the explanations, a longer immersion time of the composites led to more apatite formation which can be seen in Fig. 4(d).

In addition, as it can be seen in of high magnification SEM micrographs of composites after 1, 3 and 7 day immersion in SBF solution, immediately after immersion in SBF, small spherical micro and nanoparticles of apatite created and started to grow up on the surface of composite samples. Furthermore, after 3 and 7 day immersion in SBF, the apatite particles fully grew up and particles with plate-like nanostructure were oriented perpendicular to the surfaces of composites and distributed over the entire surfaces.

We also confirmed the formation of bone-like apatite layer on the surface of composites by EDX analysis, so the apparition of apatite formations on the surfaces of composite samples before and after immersion in SBF solution was established by EDX procedure which is shown in Fig. 4. Right after 1 day in SBF solution, EDX analysis showed an increase in P and a significant decrease in Si intensities. In addition, after 3 day immersion in SBF solution, there was a decrease in Si intensity that caused the disappearance of the Si peak, and the molar ratio of Ca–P developed to a value which was corresponded to nonstoichiometric biological apatite. After 7 day, the Ca–P molar ratio improved in the range of 1.6 which could be related to nonstoichiometric HCAp [29].

The results from EDX analysis revealed the gradual development of the nano plate-like apatite layers on the surfaces of the composites after immersion in SBF solution. Also, the disappearance of the Si peak in later days was attributed to the formation of a fully grown thicker apatite layer on the surfaces of the respective samples. Furthermore, EDX analysis showed that after 7 day immersion in SBF solution, the Ca/P ratios were in accordance to nonstoichiometric biological apatite which was approximately 1.66.

We also investigated apatite formation on the surface of composite sample containing 15% BGFs by XRD analysis which is shown in Fig. 5. In the untreated pattern, the apatite phase was observed in the compositions (apatite is the product of the setting reaction). And it is important to point out that the BGFs never prevent the conversion of reactant materials (TTCP and DCPD) to apatite phase and some small diffraction apatite peaks could be seen which were related to these conversions.

According to the previous explanations, the setting mechanisms of CPCs are so complicated that have not been identified completely but there are some hypotheses about the setting phenomena of them. The main reason for the setting process of CPCs is the precipitation of different phases such as brushite, apatite or octacalcium phosphate in the cement paste. Herein, brushite and TTCP can be clearly seen in the XRD pattern of the untreated sample.

The substance formed on the surface of the composite sample became detectable after 1 day immersion in SBF, new peaks at 26° and 32° were assigned to be (002) and (211) reflections of apatite phase according to the standard card (JCPDS file No. 09–0432). After 3 day immersion, the two peaks were intensified and the other peaks of apatite at

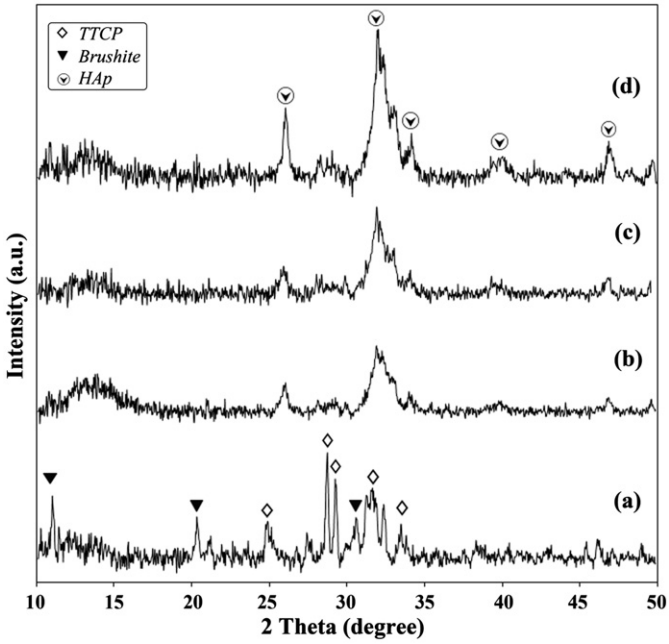

Fig. 5. The XRD patterns of the composite sample (a) before, (b) after 1 day, (c) after 3 day and (d) after 7 day immersion in SBF.

Table 1
The average crystallite size of apatite formed on the composite samples after immersion in SBF.

Immersion time (day)	Average crystallite size (nm)
1	12.10
3	16
7	17.38

28°, 40° and 46° also appeared, and finally after 7 day of immersion all of the peaks became more apparent. It is notable that the XRD patterns showed some HAp wide reflections, indicating a poor crystalline phase formation (a nearly amorphous like phase) [30].

In addition, the average nanocrystallite size of apatite formed on the composite sample containing 15% BGFs after immersion in SBF was determined from the half-width of diffraction major peaks using the Debye–Scherrer's formula (7):

$$D = k\lambda/\beta\cos\theta \quad (7)$$

where D is the crystallite diameter of, k is a constant (shape factor, about 0.9), λ is the X-ray wavelength (1.5405 Å as mentioned before), β is the full width at half maximum (FWHM) of the diffraction line, and θ is the diffraction angle.

Table 1 shows the average nanocrystallite size of apatite crystallite at various SBF immersion times. According to data from this table, the mean diameter was approximately 12.1 nm, 16 nm and 17.38 nm after 1, 3 and 7 immersion days in SBF solution, respectively. According to the data from this table, it is obvious that the increasing of immersion time (from 1 day to 7 day) caused growing of apatite crystallite.

3.3.1. In vitro osteoblastic cell attachment

Osteoblastic cells have been widely used as a model system due to their promising advantages such as world wide availability, good and well-documented characterization, the possibility to obtain large amounts of cells in a short time, and showing the entire differentiation sequence of osteoblastic cells. The latter point, particularly the ability of cells to deposit a mineralization-competent extracellular matrix (ECM), makes these cells a valuable model for studying events associated with the late osteoblastic differentiation stage in human cells. Herein, we propagated the cells over the composite samples and observed them for phenotypic properties which are shown in Fig. 6. The SEM micrographs of the cells cultured on the composites showed well-spread cells on them with numerous lamellipodia and filopodia, an indication of good attachment and penetration on the surface of the samples. The cells actively secrete ECM, which are shown with white arrows on the surfaces of samples, and ECM gave an unsmooth appearance to the cells. Naturally, the cells left traces of ECM along their migration path and wide distribution of these traces on the surfaces is an indication of good cellular migration and osteoconductivity. The continuous increase in cell aggregation during 3 day incubation indicated the ability of the prepared composites to support cell growth.

In addition, EDX anayasis was used to detect calcium deposit of cells implanted on the composite samples. It is worth mentioning that calcium and phosphorous were detected in the ECM of cells on the samples. The results obtained indicated that the prepared composite samples were good cytocompatible material that allows the adhesion, proliferation and differentiation of osteogenic cells.

3.4. Cell viability

Fig. 7 shows the function of samples with and without fibers on the viability of osteoblastic cells measured by MTT assay. There was no significant difference in formation of formazan between the control and other samples when the cells were cultured with the samples for 2 day ($p < 0.05$). However both in the 5th day, the amount of formazan production of cells for the fiber containing composite was higher than the control sample. When the fibers applied into the structure of composite more formazan was formed compared to other sample without fibers and also that of control. The results suggest that the osteoblastic cells could proliferate thoroughly in presence of fibers.

3.5. Alkaline phosphatase activity

The biocompatibility evaluation of the samples was assessed through in vitro cell culture experiments. In this

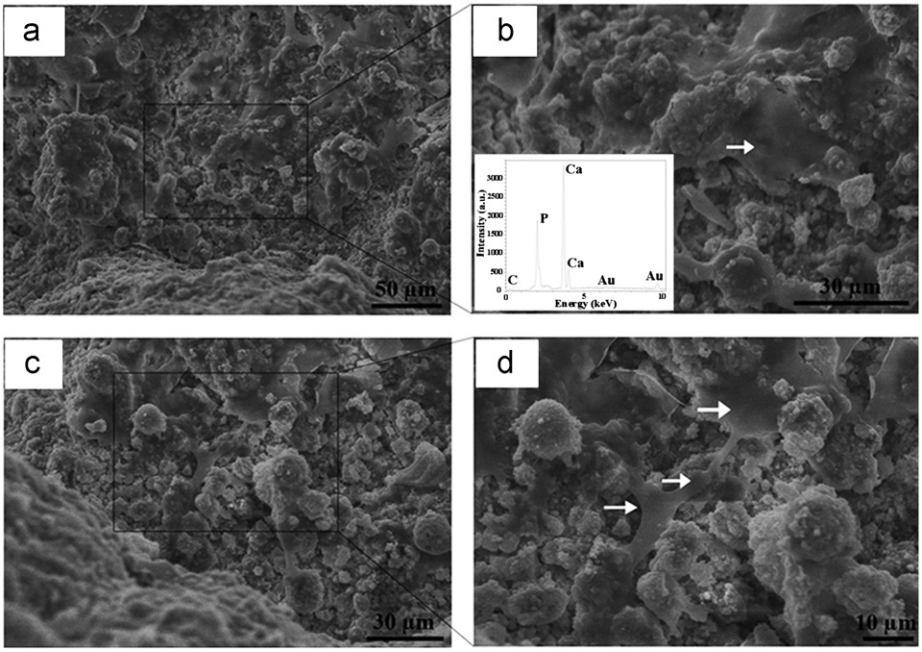

Fig. 6. Low (a) and (c), and high (b) and (d) magnifications SEM micrographs of osteoblast cells grown on the composites cell clumps; white arrows show the osteoblast cells with ECM.

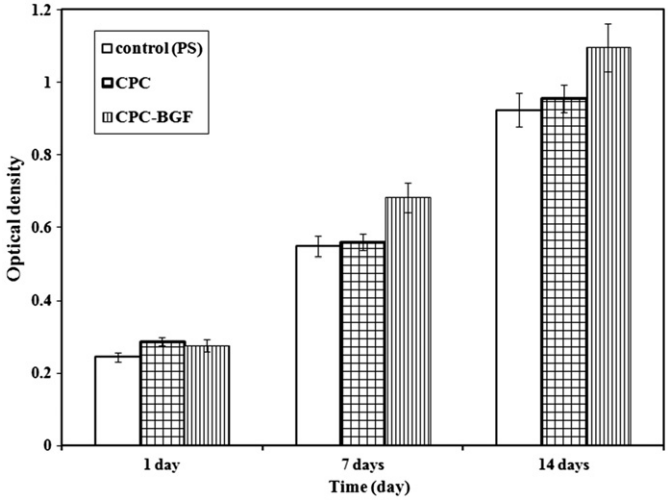

Fig. 7. Proliferation of the osteoblastic cells when culturing them with samples (*: $p < 0.05$, **: $p < 0.005$).

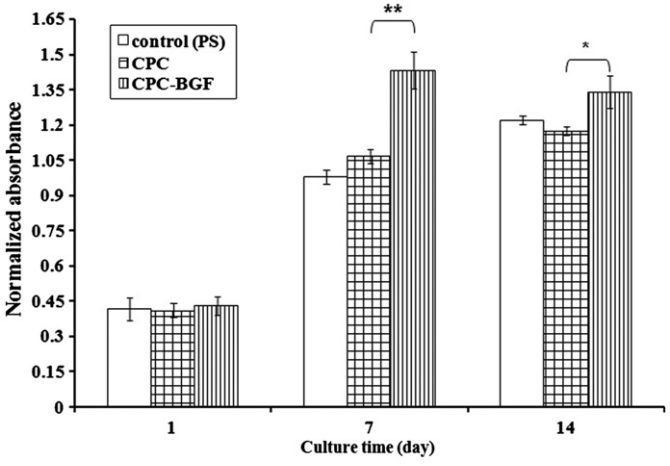

Fig. 8. ALP activity of the osteoblastic cells cultured with samples for 7 day (*: $p < 0.05$, **: $p < 0.0$).

way, we have tried to focus on alkaline phosphate activity (AP activity) of osteoblastic cells because one of the phenotypic markers for osteoblast proliferation and differentiation is alkaline phosphatase expression. The osteoblastic cells on the samples were assayed for retention of their osteoblast-like phenotype and the results are shown in Fig. 8. The level of ALP production was not statistically different for all specimens at the 1st day. At the 7th day, the cell activity on the fiber containing composite was higher than that of other specimens and approximately the same level of ALP was observed for the control and the sample without fibers. At the 14th day, the growth level of the cells on the fiber containing sample was again higher than that of other specimens ($p > 0.05$) and in all days the maximum cell activity was observed on this sample.

4. Conclusion

In conclusion, the incorporation of BGFs into the CPC paste caused improved mechanical properties. The optimum amount of the fibers which successfully improved the compressive strength, modulus and toughness of the CPC was 15 wt% based on the total weight of the cement powder and liquid. In addition, the biomineralization studies of the mechanically optimized composite sample in SBF solution showed that the deposition bone-like apatite phase on the

surface of the composites ascertaining the bioactive nature of the prepared samples. Finally, it was proved that the prepared CPC/BGFs composite was non-toxic and biocompatible for the proposed work in segmental defects and the experiments provided data to support the use of the composite in bone repair applications.

Acknowledgment

The authors would like to thank many colleagues, Ph.D. students and collaborators who have made a vast contribution to this area of research.

References

[1] J.F. Osborn, H. Newesely, The materials science of calcium phosphate ceramics, Biomater 1 (1980) 108–111.
[2] L.L. Hench, Bioceramics, Journal of American Ceramic Society 81 (1998) 1705–1728.
[3] K. Ishikawa, S. Takagi, L.C. Chow, Y. Ishikawa, Properties and mechanisms of fast setting calcium phosphate cements, Journal of Material Science: Materials in Medicine 6 (1995) 528–533.
[4] M. Mami, A. Lucas-Girot, H. Oudadesse, R. Dorbez-Sridi, F. Mezahi, E. Dietrich, Investigation of the surface reactivity of a sol gel derived glass in the ternary system SiO_2–CaO–P_2O_5, Applied Surface Science 254 (2008) 7386–7393.
[5] Y. Doi, T. Shibutani, Y. Moriwaki, T. Kajimoto, Y. Iwayama, Sintered carbonate apatites as bioresorbable bone substitutes, Journal of Biomedical Materialas Research Part A 39 (1998) 603–610.
[6] J.E. Barralet, S.M. Best, W. Bonfield, in: P. Ducheyne, D. Christiansen (Eds.), Preparation and sintering of carbonate substituted apatite in Bioceramics, vol. 6, Butterworth-Heinemann Ltd., Oxford, 1993, pp. 179–184.
[7] B.R. Constanz, I.C. Ison, M.T. Fulmer, R.D. Fulmer, R.D. Poser, S.T. Smith, M Vanwagoner, J Ross, SA Goldstein, JB Jupiter, DI. Rosental, Skeletal repair by in situ formation of the mineral phase of bone, Science 267 (1995) 1796–1799.
[8] D.C. Greenspan, J.P. Zhong, G.P. Latorre, Effect of surface area to volume ratio on in vitro surface reactions of bioactive glass particulates, Bioceramics 7 (1994) 28–35.
[9] A. Balamurugan, G. Sockalingum, J. Michel, J. Fauré, V. Banchet, L. Wortham, S. Bouthors, D. Laurent-Maquin, G. Balossier, Synthesis and characterisation of sol gel derived bioactive glass for biomedical applications, Materials Letter 60 (2006) 3752–3757.
[10] S. Saha, S. Pal, Improvement of mechanical properties of acrylic bone cement by fiber reinforcement, Journal of Biomechanics 17 (1984) 467–478.
[11] B. Pourdeyhimi, H.H. Robinson, P. Schwartz, H.D. Wagner, Fracture toughness of Kevlar 29/poly(methyl methacrylate) composite materials for surgical implantations, Annals of Biomedical Engineering 14 (1986) 277–294.
[12] B. Pourdeyhimi, H.D. Wagner, Elastic and ultimate properties of acrylic bone cement reinforced with ultra-high-molecular-weight polyethylene fibers, Journal of Biomedical Materials Research 23 (1989) 63–80.
[13] N.H. Ladizesky, Y.Y. Cheng, T.W. Chow, I.M. Ward, Acrylic resin reinforced with chopped high performance polyethylene fiber-properties and denture construction, Dental Materials 9 (1993) 128–135.
[14] BR. Lawn, Fracture of Brittle Solids, Cambridge University Press, London, 1993 chapter 8.
[15] N. Nezafati, F. Moztarzadeh, S. Hesaraki, M. Mozafari, Synergistically reinforcement of a self-setting calcium phosphate cement with bioactive glass fibers, Ceramics International 37 (2010) 927–934.
[16] T. Kokubo, H. Takadama, How useful is SBF in predicting in vivo bone bioactivity?, Biomaterials 27 (2006) 2907–2915
[17] A. Oyane, H.M. Kim, T. Furuya, T. Kokubo, T. Miyazaki, T. Nakamura, Preparation and assessment of revised simulated body fluids, Journal of Biomedical Materials Research 65A (2003) 188–195.
[18] H. Takadama, M. Hashimoto, M. Mizuno, T. Kokubo, Round-robin test of SBF for in vitro measurement of apatite-forming ability of synthetic materials, Phosphrus Research Bulletin 17 (2004) 119–125.
[19] S. Hesaraki, M. Gholami, S. Vazehrad, S. Shahrabi, The effect of Sr concentration on bioactivity and biocompatibility of sol–gel derived glasses based on CaO–SrO–SiO_2–P_2O_5 quaternary system, Materials Science and Engineering C 30 (2010) 383–390.
[20] LA Dos Santos, RG Carrodeguas, AO Boschi, ACF. de Arruda, Fiber-enriched double-setting calcium phosphate bone cement, Journal of Biomedical Materials Research Part A 65A (2003) 244–250.
[21] M Mozafari, F Moztarzadeh, Investigation of the physico-chemical reactivity of a mesoporous bioactive SiO_2–CaO–P_2O_5 glass in simulated body fluid, Journal of Non-Crystalline Solids 356 (2010) 1470–1478.
[22] M Mozafari, F Moztarzadeh, M Rabiee, M Azami, N Nezafati, Z Moztarzadeh, Development of 3D bioactive nanocomposite scaffolds made from gelatin and nano bioactive glass for biomedical applications, Advanced Composites Letters 19 (2010) 91–96.
[23] S Hesaraki, F Moztarzadeh, D. Sharifi, Formation of interconnected macropores in apatitic calcium phosphate bone cement with the use of an effervescent additive, Journal of Biomedical Materials Research 83 (2007) 80–87.
[24] M Komath, KH Varma, R. Sivakumar, On the development of an apatitic calcium phosphate bone cement, Bulletin of Material Science 23 (2000) 135–140.
[25] XX Yan, CZ Yu, XF Zhou, JW Tang, DY. Zhao, Highly or- dered mesoporous bioactive glasses with superior in vitro bone-forming bioactivities, Angewandte Chemie International Edition 43 (2004) 5980–5984.
[26] C. Benaqqa, J. Chevalier, M. Saadoui, G. Fantozzi, Slow crack growth behaviour of hydroxyapatite ceramics, Biomaterials 26 (2005) 6106–6112.
[27] N. Rameshbabu, T.S.S. Kumar, K. Prasad Rao, Synthesis of nanocrystalline fluorinated hydroxyapatite by microwave processing and its in vitro dissolution study, Bulletin of Material Science 29 (2006) 611–615.
[28] M Mozafari, M Rabiee, M Azami, S. Maleknia, Biomimetic formation of apatite on the surface of porous gelatin/bioactive glass nanocomposite scaffolds, Applied Surface Science 257 (2010) 1740–1749.
[29] G.A. Stanciu, I. Sandulescu, B. Savu, S.G. Stanciu, K.M. Paraskevopoulos, X. Chatzistavrou, E. Kontonasaki, P. Koidis, Investigation of the hydroxyapatite growth on bioactive glass surface, Journal of Biomedical and Pharmaceutical Engine 1 (2007) 34–39.
[30] P. Li, I. Kangasniemi, K. de Groot, T. Kokubo, Bonelike Hydroxyapatite Induction by a gel-derived titania on a titanium substrate, Journal of American Ceramic Society 77 (1994) 1307–1312.